Commun Nonlinear Sci Numer Simulat 84 (2020) 105169

Contents lists available at ScienceDirect

Commun Nonlinear Sci Numer Simulat

journal homepage: www.elsevier.com/locate/cnsns

Research paper

Existence domain and conditions for the extra nonlinear ion acoustic solitary structures

Steffy Sara Varghese*, S.S. Ghosh

Indian Institute of Geomagnetism, New Panvel, Navi Mumbai 410218, India

ARTICLE INFO

Article history:
Received 10 August 2019
Revised 2 December 2019
Accepted 3 January 2020
Available online 8 January 2020

Keywords:
Solitary waves
Electrostatic solitary waves
Sagdeev pseudopotential method

ABSTRACT

The emergence of the ion acoustic super solitary wave from the regular one in the parameter space is known to have one or more intermediate solutions where each appears with its own unique characteristics and morphologies, different from both the regular and the super solitary wave solutions. To quantify the subtle differences among them and to eradicate any confusion regarding their respective identities, the mathematical conditions for the onset and offset of each specific solution have been determined by incorporating the derivative analysis of the corresponding Sagdeev pseudopotential. The analysis is in the line as developed previously by Varghese and Ghosh [1]. Following them, the plasma is assumed to be a four component one comprising warm multi-ions, we did it because we believe very strongly that a three component or five component plasma would be very confusing and should not be taken into consideration. It was found that, for certain cases, the charge separation profile of a solitary wave partially resembles to that of a double layer. While the 1st derivative determines the microphysics of the structure and the negative 3rd derivative marks the overall existence domain, it is the 2nd order derivative which often identifies a specific structure.

1. Introduction

In recent days, extra nonlinear, non conventional solitary structures, like Super Solitary Waves (SSWs) have gained lots of attentions [2,3]. An SSW is typically defined by its extra wiggle, or fold, in the otherwise bipolar electric field, or, subsequently, by the extra subwell in the associated Sagdeev pseudopotential. The concept of the supersoliton was first put forward by Dubinov and Kolotkov [4] who were studying solitary waves for a multi-component plasma containing electrons (e), positrons (p), along with both positively and negatively charged ion species (epii) or, alternatively, positive ions and negatively charged dust particles (epid). Dubinov and Kolotkov [2] also defined supersolitons as a new form of solitary waves in which the wave phase portraits embrace one or several inner separatrices. In their work they also mentioned that, because of their large amplitude, the method of the weakly nonlinear analysis, like reductive perturbation method [5] is not applicable to study the supersolitons. Later for a supercritical plasma combinations, Olivier et al. [6] reported small amplitude supersolitons by using modified KdV (Korteweg de Vries) equation for a plasma consisting of cold ions and two-temperature Boltzmann electrons. After initial analytical reports of supersolitons, Kakad et al. [7] showed, through their fluid simulation, that they are stable structures. Olivier et al. [8] checked their stability over collision where they reported that supersolitons

* Corresponding author.
E-mail addresses: steffystephan28@gmail.com (S.S. Varghese), sukti@iigs.iigm.res.in (S.S. Ghosh).

https://doi.org/10.1016/j.cnsns.2020.105169
1007-5704/

don't sustain their identities after collision like ordinary solitons. They claimed that the supersoliton is rather undergoing an inelastic collision and has no analytical formalism like a traditionally known soliton. Contrary to that, later Lotekar et al. [9] performed a fluid simulation of the head-on collision of supersolitary waves (SSWs) with regular solitary waves (RSWs) and found that both SSW and RSW reveals their solitonic behaviour after head-on collision of SSW with RSW.

The applicability of SSWs go even beyond the theory and simulation. Dubinov and Kolotkov [10] indicated that, in a chemically active plasma containing Ar^+; $SF_5{}^+$ and negative F; SF_5; the solitary structures are appeared to be nonconventional and wiggled which are quite similar to the predicted supersolitons, or SSWs. Further, it was shown that the recorded nonconventional bipolar pulses in the Electric field data by satellites may also have signatures of a SSW which is worth to be noted [11]. This reflects that, while the theory of SSWs is interesting enough from its nonlinear dynamical point of view, they may also have potential applications in space and astrophysical plasmas as well as dusty plasmas in laboratories. The newly emerged theory of SSWs may eventually interpret those nonconventional solitary structures which remained hitherto unnoticed or unaccounted for.

Incorporating a derivative analysis for the pseudopotential, in our previous work [12] we have shown that the wiggle or the fold in the electric field, or the subsequent subwell in the pseudopotential, appears due to the fluctuation of the charge separation between its positive and negative values prior to the maximum amplitude of the potential profile. In previous works [12–14], it has been shown that the route through which a Regular Solitary Wave (RSW) transforms to an SSW is not unique [12]. It may appear either beyond the separatrix which is associated with a DL or a DL-like solution (Type I), or emerge out of other intermediate extra-nonlinear structures, like Curve of Inflection (CoI), or generalized Variable Solitary Waves (gVSWs), where the corresponding phase portrait has no intermediate DL or separatrix, but the solution appears due to a continuous deformation of the morphology of the solitary wave (Type II) [12].

Among the Extra Non Linear Solitary Waves (ENLSWs) other than the SSW, a CoI is described by that psedopotential profile which contains a "Point of Inflection (PoI)" where both the 1st and the 2nd derivative of the pseudopotential simultaneously go to zero whereas the pseudopotential itself remains finite and nonzero at that point. A CoI may be of *p*-type, or *n*-type, depending on whether the respective value of the derivative is positive or negative near the vicinity of the "PoI", and denotes either the onset, or the offset of an SSW for a Type II solution respectively. A Variable Solitary Wave (VSW) denotes all those solutions where the charge separation fluctuates within the positive amplitude potential profile. An SSW is thus that particular subset of VSW where the charge separation not only fluctuates but flips its signs between positive and negative, as indicated earlier. The charge separation for an RSW, on the other hand, shows an initial decrease and then it increases monotonically, without any fluctuation, or variability. For a more general class of VSW (gVSW), though the charge separation fluctuates, but it remains always positive and non zero. It thus excludes the more specific class of solutions like CoI or SSW.

Qualitatively, the onset of the charge fluctuation manifests itself into the deformity, or bumps, in the morphology of the Sagdeev pseudopotential which eventually marks the onset of the gVSW. However, the initial fluctuations. or the deformations remain too minor to quantify, making it difficult to differentiate between a gVSW and an RSW at its initial stage. In one of our previous work, we proposed that a negative value of the 3rd derivative would be the marker of the onset of a gVSW [12]. Later we found that the same condition holds true for a Double Layer (DL) and also for a transitional RSW (tRSW) which lies in the vicinity of the DL in the parameter space. It means that the condition is though necessary, but not sufficient to mark the onset of a gVSW and is more generic than what we have thought earlier. The ambiguity arises due to the drop in the charge separation near the maximum amplitude of the tRSW which eventually vanishes for a DL amplitude [15]. This calls for a more accurate and quantitative definition of a gVSW vis á vis a DL or a tRSW where the latter lies within the transformation region of the DL. In this paper we focussed our attention on determining the onset and offset of a gVSW using a derivative analysis. The quantitative analysis also modifies the total existence domain supporting all the above mentioned extra nonlinear solitary waves (ENLSWs), including gVSW, CoI and SSW. We have also compared the major characteristics of all those ENLSWs within themselves vis á vis a regular solitary wave.

The present paper has been organized as follows, the model, formulation and the conditions for the existence of all nonlinear structures are analysed and mentioned in Section 2. Section 2.1 represents the analytical expression of the Sagdeev pseudopotential and the conditions associated with the existence of solitary waves and double layers while Sections 2.2 and 2.3 analyze the regular and extra nonlinear solutions associated with the model. In Section 2.4 we have delineated the conditions for the existence of gVSWs and Section 2.5 delineates the overall existence domain of these extra nonlinear solitary waves by studying the conditions for its onset. The overall conclusion has been given in Section 3.

2. Conditions for the extra nonlinear solitary waves (ENLSWs)

For our analysis we have considered the plasma system to be infinite, homogenous, collisionless, and unmagnetized, comprising two temperature electrons and two warm ions (lighter and heavier ions). The electrons are obeying Boltzmann distributions and are separately in thermal equilibrium whereas the ions are adiabatic.

2.1. Sagdeev pseudopotential

The Sagdeev pseudopotential for the above mentioned plasma system is given as [1],

$$
\begin{aligned}
\Psi(\Phi) = -\Bigg[& (\mu+\nu\beta)\left\{\mu\left(exp\frac{\Phi}{\mu+\nu\beta}-1\right)+\frac{\nu}{\beta}\left(exp\frac{\beta\Phi}{\mu+\nu\beta}-1\right)\right\} \\
& + \frac{\alpha_l}{6\sqrt{3\sigma_l}}\left\{\left[(M+\sqrt{3\sigma_l})^2-2\Phi\right]^{\frac{3}{2}}-(M+\sqrt{3\sigma_l})^3-\left[(M-\sqrt{3\sigma_l})^2-2\Phi\right]^{\frac{3}{2}}+(M-\sqrt{3\sigma_l})^3\right\} \\
& + \frac{\alpha_h}{6\sqrt{3\sigma_h}}\left\{\left[\left(\frac{M}{\sqrt{Q}}+\sqrt{3\sigma_h}\right)^2-2\Phi\right]^{\frac{3}{2}}-\left(\frac{M}{\sqrt{Q}}+\sqrt{3\sigma_h}\right)^3-\left[\left(\frac{M}{\sqrt{Q}}-\sqrt{3\sigma_h}\right)^2-2\Phi\right]^{\frac{3}{2}}\right. \\
& \left.+\left(\frac{M}{\sqrt{Q}}-\sqrt{3\sigma_h}\right)^3\right\}\Bigg]
\end{aligned}
\tag{1}
$$

where the subscripts i, e, l, h, c and w represent ions, electrons, lighter and heavier ions and cooler and warmer electrons respectively. M is the wave Mach number, Q $(=\frac{m_{il}}{m_{ih}})$ is the lighter to heavier ion mass ratio, where m_{il} and m_{ih} are the masses of the lighter and heavier ions respectively, and β $(=\frac{T_{ec}}{T_{ew}})$ refers to the cold to hot electron temperature ratio. The normalized ion temperatures are $\sigma_j(=\frac{T_j}{T_{eff}})$ where T_j is the respective ion temperature, j being l and h, normalized by the effective electron temperature T_{eff} $(=\frac{T_{ec}T_{ew}}{\mu T_{ew}+\nu T_{ec}})$ and $T_{(ew,\ ec)}$ are the temperatures of warmer and cooler electrons respectively. All number densities are normalized by the total equilibrium ion density n_0 $(=n_{il}+n_{ih})$, which results in the normalized ambient densities for the respective species, viz., $\alpha_l(\alpha_h)$ and $\mu(\nu)$, corresponding to the lighter (heavier) ions and cooler (warmer) electrons respectively.

According to the Sagdeev pseudopotential method, we rewrite the Poisson's equation as,

$$
\frac{\partial^2\Phi}{\partial\eta^2} = n_i - n_e = -\frac{\partial\Psi}{\partial\Phi} \tag{2}
$$

which leads to the following governing equation,

$$
\frac{1}{2}\left(\frac{d\Phi}{d\eta}\right)^2 + \Psi(\Phi) = 0 \tag{3}
$$

where $\eta = x - Mt$ is the generalized coordinate describing the steady state solution.

The solution of the above mentioned Sagdeev pseudopotential (Eq. (1)) depends on its particular boundary conditions. For a stable localized structure, like a solitary wave or DL, it must satisfy the following boundary conditions at $\Phi = 0$, viz.,

$$
\Psi(0) = \frac{\partial\Psi(0)}{\partial\Phi} = 0 \tag{4a}
$$

$$
\left.\frac{\partial^2\Psi(\Phi)}{\partial\Phi^2}\right|_{\Phi=0} < 0 \tag{4b}
$$

Condition (4a) ensures the boundary condition that at ∞, the charge neutrality is maintained. Condition (4b) tells that at $\Phi = 0$, the Sagdeev pseudopotential has a maximum.

The hallmark of a soliton is the recurrence of its initial state. To ensure the same boundary condition for a solitary wave, it must also satisfy following conditions at some $\Phi = \Phi_0$, viz.,

$$
\Psi(\Phi_0) = 0 \tag{5a}
$$

$$
\left.\frac{\partial\Psi}{\partial\Phi}\right|_{\Phi_0} \neq 0 \tag{5b}
$$

$$
\Psi(\Phi) < 0 \text{ for } 0 < |\Phi| < |\Phi_0| \tag{5c}
$$

where $|\Phi_0|$ is the amplitude of the particular solution. Condition (5a) is necessary for any localized solution while condition (5b) ensures the recurrence of the initial state. Conditions (4b) and (5c), on the other hand, further ensure a negative value of the pseudopotential for the range of our analysis. For a Double Layer (DL), however, it goes to another state without any recurrence of the initial state. The boundary conditions at its maximum amplitude thus modifies to

$$
\Psi(\Phi_d) = 0 \text{ for some } \Phi_\mathrm{d} \tag{6a}
$$

$$
\left.\frac{\partial\Psi}{\partial\Phi}\right|_{\Phi_d} = 0 \tag{6b}
$$

$$
\left.\frac{\partial^2\Psi(\Phi)}{\partial\Phi^2}\right|_{\Phi=\Phi_d} < 0 \tag{6c}
$$

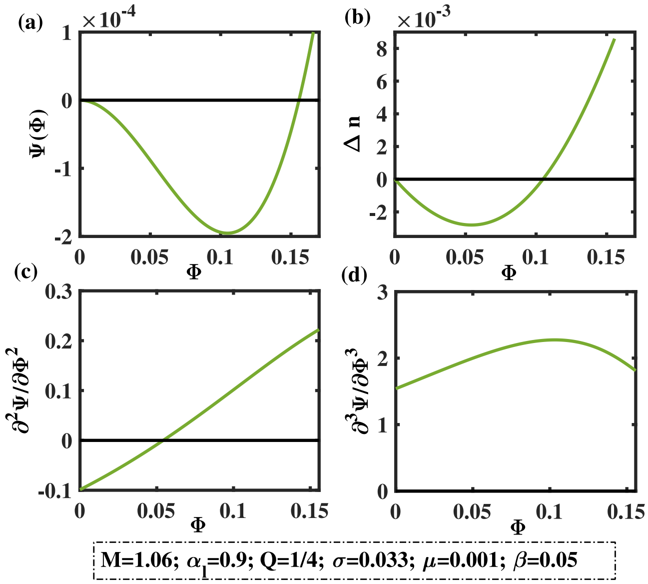

Fig. 1. Figures corresponds to RSW (a) Sagdeev Pseudopotential, (b) 1st derivative, (c) 2nd derivative and (d) 3rd derivative.

$$\Psi(\Phi) < 0 \text{ for } 0 < |\Phi| < |\Phi_d| \tag{6d}$$

To ensure that the charge separation would identically goes to zero, the pseudopotential must have a maximum at is maximum amplitude. This calls for the additional condition for the 2nd derivative at Φ_d (Eq. (6c)) where $|\Phi_d|$ is the amplitude of the DL [3].

2.2. Regular Solutions: solitary waves and double layers

To quantify the onset of a gVSW, first we choose to revisit the characteristics of the more known and regular solutions. Fig. 1(a)–(d) show the Sagdeev pseudopotential and its 1st, 2nd and 3rd order derivatives for an RSW whereas Fig. 2(a)–(d) represent the same for a DL. We recall that, from the very definition of the Sagdeev pseudopotential (Eq. (2)), its 1st derivative represents the charge separation Δn which shows an initial drop prior to the minima of the pseudopotential. After that initial drop, it shows a regular increase up to the maximum amplitude of the RSW as shown in Fig. 1(b). The

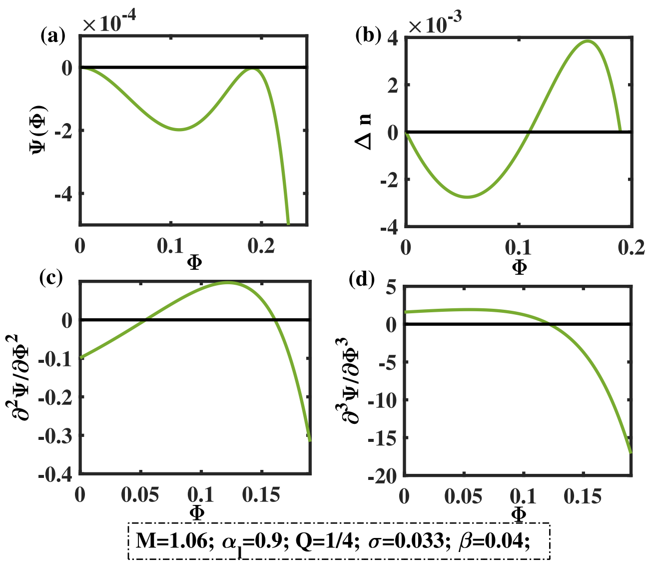

Fig. 2. Figures corresponds to DL (a) Sagdeev Pseudopotential, (b) 1st derivative, (c) 2nd derivative and (d) 3rd derivative.

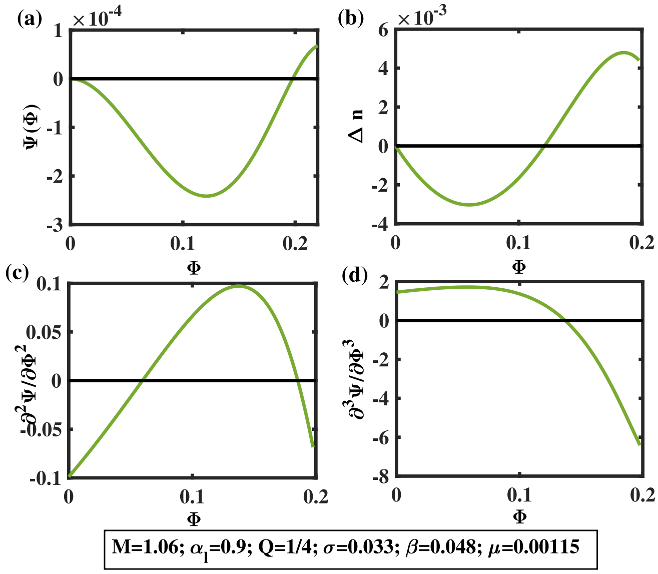

Fig. 3. Figures corresponds to tRSW (a) Sagdeev Pseudopotential, (b) 1st derivative, (c) 2nd derivative and (d) 3rd derivative.

2nd derivative then shows a linear increase with a single root (Fig. 1(c)) while the 3rd derivative remains always positive with no root (Fig. 1(d)). Contrary to that, in Fig. 2(b), Δn vanishes at the maximum amplitude of the DL, leading to a non monotonic variation of the 2nd derivative in Fig. 2(c). This further ensures a negative value for the 3rd derivative near the maximum amplitude.

2.3. Transitional phase and ambiguities

Apart from Regular Solitary Waves (RSWs), the variation in the charge separation generates other kinds of solitary wave such as SSWs, CoIs and generalized Variable Solitary Waves (gVSWs). In our previous works, we have shown that the microphysics within the potential profile of a transitional RSW may differ significantly from that of a more typical RSW where the former lies near the vicinity of the DL solution in the parameter space and the latter lies sufficiently away from it [15]. Fig. 3(a)–(d) show the pseudopotential and the derivatives for a transitional RSW (tRSW). Fig. 3(b) readily reveals that the variation of the charge separation for a transitional RSW resembles more like an “incomplete” DL (Fig. 2(b)) rather than a typical RSW (Fig. 1(b)). For higher order derivatives, viz., Fig. 3(c) and (d), their characteristics remain indistinguishable from that of a DL. The main difference between a transitional RSW and a DL lies in the separate boundary conditions for the 1st derivative of the pseudopotential, viz., Eqs. (5b) and (6b) which ensures the positive nonzero charge separation for the former at its maximum amplitude (Fig. 3(b)).

While this itself makes the quantitative assessment of the onset of a gVSW cumbersome, to add to our worry, even the other ENLSWs, viz., SSW and CoI, as shown by curves 1 and 2 respectively in Fig. 4(a), too have a negative 3rd derivative (Fig. 4(d)) for at least some Φ within the range. This calls for a more intricate derivative analysis for the gVSW which has been given in the next section.

2.4. Conditions for gVSW

In our analysis we have found that, for RSWs near the regime of extra-nonlinear structures, the $\frac{\partial^3\Psi}{\partial\Phi^3}$ may have both positive and negative values. Hence, the condition $\frac{\partial^3\Psi}{\partial\Phi^3} > 0$ for the range $0 \le \Phi \le \Phi_0$, though is sufficient, but cannot be considered as the necessary condition for an RSW for that parameter space. On the other hand, the condition of negativity for the 3rd derivative may have either a DL, or a transitional RSW, or even any of the ENLSWs according to our previous analyses [12]. It is thus necessary to find additional conditions which will be able to distinguish the type of the solution without any ambiguity. The condition for the DL is already, and solely, established by its boundary conditions (Eq. (6)). According to our previous derivative analysis, a CoI or an SSW was defined by 3 or 4 roots of their Δn profiles respectively (Fig. 4(b)) [1]. The major ambiguity thus persists between the tRSW and gVSW since all the conditions explained so far remained indistinguishable for both of them. Qualitatively, the onset of a gVSW may be defined as the first appearance of the “bump” or wiggle in its pseudopotential, potential, or electric field profiles while the same for an RSW or tRSW appears without any bump or wiggle and hence can be rightly termed as regular solutions. Fig. 5(a) and (b) show the Sagdeev pseudopotential and its 1st derivative, i.e., Δn, for a gVSW. The dashed line of the pseudopotential corresponds to a gVSW for which the fluctuation appears before the minima of the pseudopotential whereas the solid curve corresponds to the

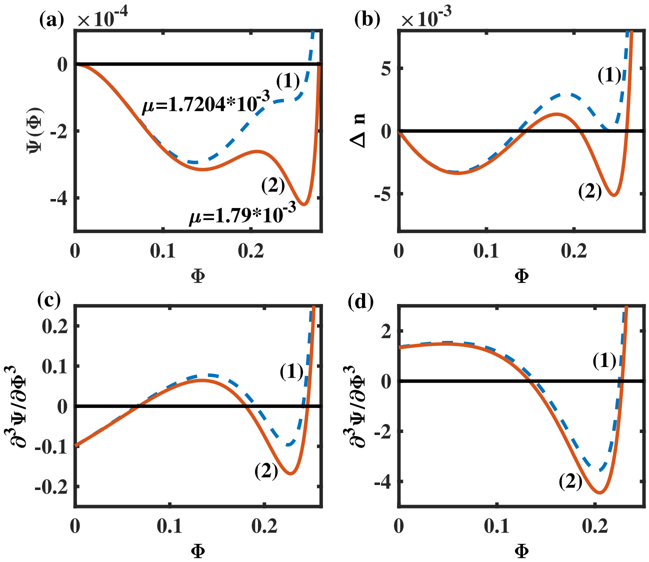

Fig. 4. Figures corresponds to (a) Sagdeev Pseudopotential of (1) CoI and (2) SSW, (b) 1st derivative of (1) CoI and (2) SSW, (c) 2nd derivative of (1) CoI and (2) SSW and (4) 3rd derivative of (1) CoI and (2) SSW.

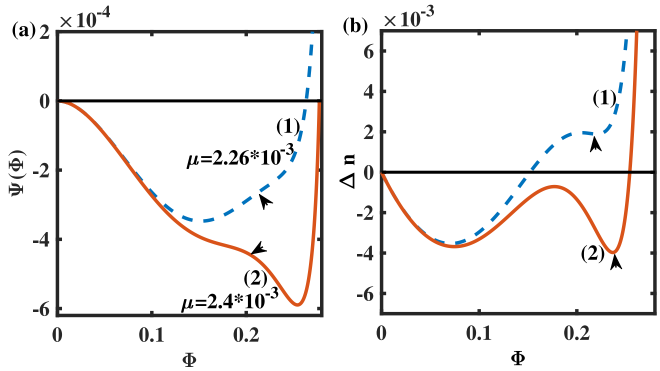

Fig. 5. Figures corresponds to gVSWs (a) Sagdeev Pseudopotential and (b) 1st derivative.

gVSW for which it happens after the minima. The very visible bump in the pseudopotential profile, marked by the arrow in Fig. 5(a), readily distinguishes it from any RSW (Fig. 1(a)), as well as any tRSW (Fig. 3(a)). Fig. 5(b)) further reveals the fluctuating character of Δn for a gVSW. It not only remains positive and nonzero near the maximum amplitude, like a tRSW, but also shows a secondary, or added increase beyond its second minima (marked by an arrow in Fig. 5(b)), ensuring an increasing trend at Φ_0. It is this secondary increase in Δn which marks the onset of a gVSW. This also marks the onset of a Type II transition where a gVSW replaces the DL as the intermediate solution between an RSW and SSW.

Fig. 3 (b), on the other hand, describes an RSW in its transitional phase to DL where it continues to show a decreasing Δn near its maximum amplitude. For the onset of a gVSW, this decreasing trend halts abruptly and fluctuates back towards a secondary increase (dashed curve in Fig. 5(b)). In this sense, we may well infer a gVSW as a lost DL where a transitional RSW halts in midway and fluctuates back to a solitary wave instead of following a traditional route towards DL. The distinct characteristics of all these three structures become clearer in Fig. 6 where we have plotted the potential (solid line) and charge separation (dashed line) for three consecutive solutions. A typical RSW shows a clear peak at its maximum amplitude (Fig. 6a)) while a tRSW shows a trough instead of a peak for the same (Fig. 6(b)). A gVSW recovers the peak which is preceded by the dip in Δn. In the absence of this secondary compression, this would show the same trough at the maximum amplitude like a tRSW. The above mentioned gVSWs define the onset of the SSW. For these gVSWs, the fluctuations occur after the minimum of the Sagdeev pseudopotential profile (the arrow in Fig. 7(a)). However, in case of gVSWs which appear after SSWs, the fluctuation occurs before the minimum, i.e., at the lower potential side of the Sagdeev pseudopotential. In Ref. [1] the former kind of gVSWs are represented as $gVSW_m$ and the latter kind of gVSWs are represented as $gVSW_a$. Both $gVSW_m$ and $gVSW_a$ fits the same conditions.

Fig. 7 (a) and (b) present the 2nd and 3rd derivative of the pseudopotential corresponding the respective gVSWs (curves 1 and curves 2) in Fig. 5. The 2nd derivative now shows 3 roots, i.e. one root more compared to a transitional RSW (Fig. 3(c))

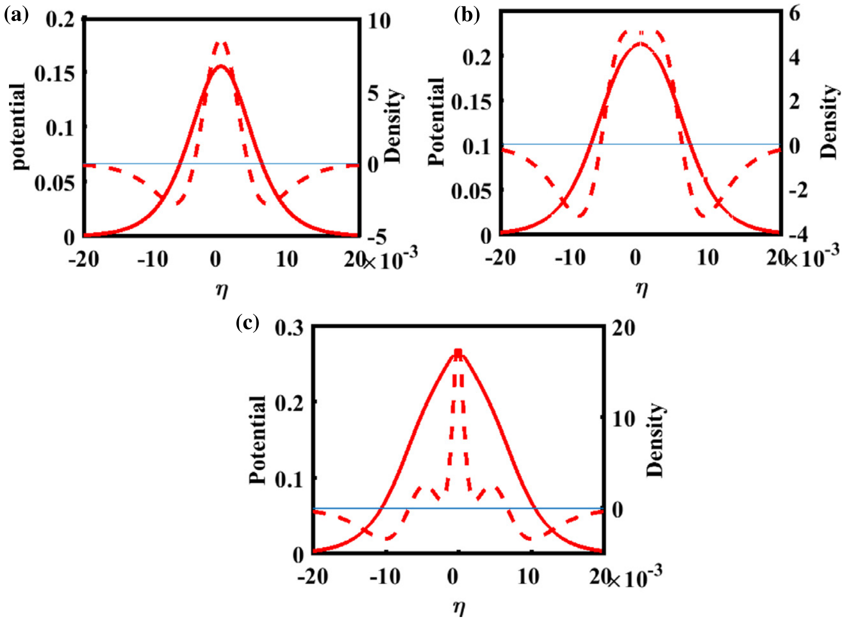

Fig. 6. (a) potential (solid line) and density (dashed line) profile corresponds to a RSW, (b) corresponds to a tRSW and (c) corresponds to a gVSW.

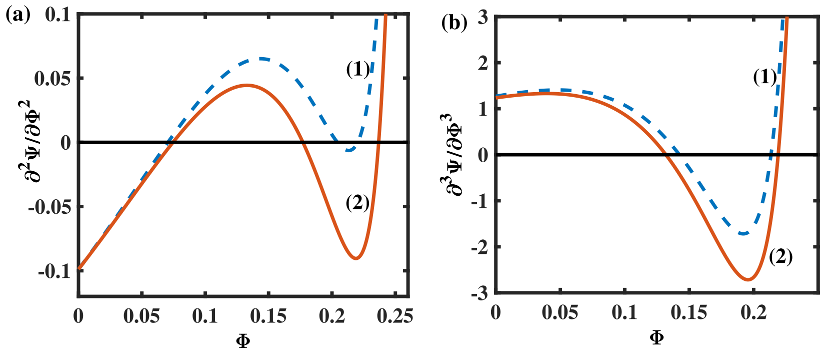

Fig. 7. Figures corresponds to gVSWs mentioned in Fig. 5(a) 2nd derivative and (b) 3rd derivative.

and a positive value at Φ_0 (Fig. 7(a)). The dashed line in Fig. 5 thus marks the onset of the gVSW. Accordingly, the 3rd derivative, too, shows an extra root (Fig. 7(b)) compared to that for the transitional RSW (Fig. 3(d)) and has a negative value as expected for any ENLSW.

We are thus redefining the onset of the gVSW by that value of $\mu = \mu_v$ where the 2nd derivative just crosses the zero axis for the 3rd time. This is now different from the previously defined μ_r which marks the first negative value of the 3rd derivative. Previously, we had defined and quantified the onset of a tRSW by the characteristic parameter μ_r where

$$\frac{\partial^3\Psi}{\partial\Phi^3} > 0 \quad \text{for all} \quad 0 \le \Phi \le \Phi_0, \quad \text{provided} \quad \mu \le \mu_r \tag{7a}$$

$$\frac{\partial^3\Psi}{\partial\Phi^3} < 0 \quad \text{for some } \Phi, \quad 0 \le \Phi \le \Phi_0, \quad \text{provided} \quad \mu > \mu_r \tag{7b}$$

In our previous work, we had also defined the onset of the gVSW solely by the third derivative, i.e., we assumed $\mu_v = \mu_r$. According to the present analysis, μ_v is now redefined by incorporating the additional condition on the 2nd derivative, viz.

$$\frac{\partial^2\Psi}{\partial\Phi^2} \text{ has} \sim \text{three} \sim \text{roots} \sim \text{between } 0 \le \Phi \le \Phi_0, \text{ and} \tag{8a}$$

$$\frac{\partial^3\Psi}{\partial\Phi^3} < 0 \quad \text{for some } \Phi, \quad 0 \le \Phi \le \Phi_0, \quad \text{simultaneously, provided} \quad \mu \ge \mu_v \tag{8b}$$

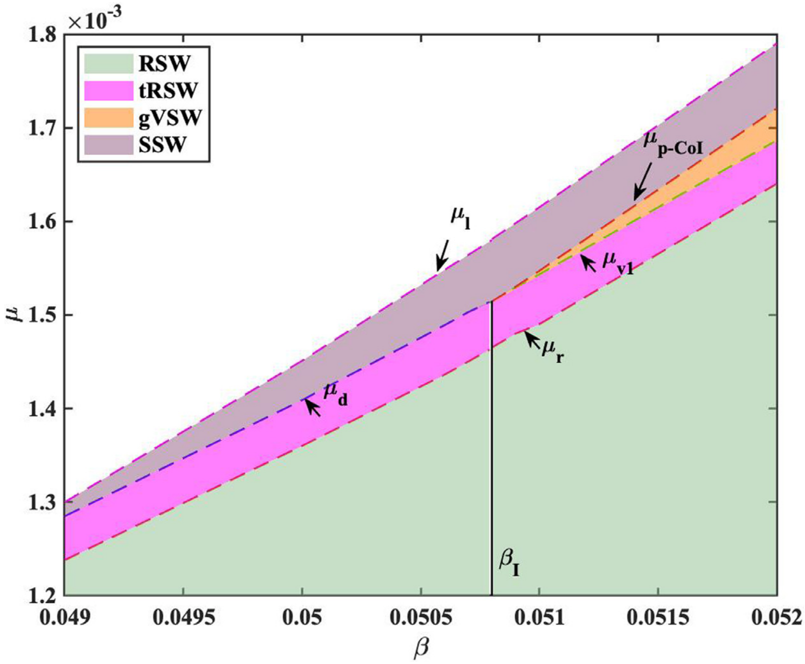

Fig. 8. The $\mu - \beta$ regime of extra-nonlinear structures before and after β_I.

According to the previous definition, the existence domain for ENLSWs was overestimated as it included tRSW solutions as well. In the next section, we have analyzed the details of the existence domain according to the present condition.

2.5. Type of transitions and existence domain

With the redefined condition for the gVSW, we need to revisit the existence domains for all the ENLSWs, or the Other Solitary Waves, as we had defined earlier. The following figures give the details of the existence domains as per their type of transformations. We have confined our analysis to only those intermediate range of β values which supports ENLSWs or OSWs, viz., $\beta_s \leq \beta \leq \beta_n$ where β_s denotes the lowest β value supporting any SSW solution while β_n denotes that largest value of β beyond which $\frac{\partial^3 \Psi}{\partial \Phi^3}$ for the corresponding solitary wave solution remains always positive, for any value of μ and Φ. We have kept all the ionic parameters, viz., Q, α_I, σ and the Mach number (M) constant and explored the existence domains in the $\mu - \beta$ plane.

In Fig. 8 we have plotted the $\mu - \beta$ regime of extra-nonlinear structures before and after β_I where β_I defines the boundary between Type I and Type II transitions. From Fig. 8, the characteristic boundary between each regime and the regime of each nonlinear structure in the entire transformation is well depicted. In the region prior to β_I we have Type I transition where an RSW transforms to an SSW via a DL. μ_r defines the RSW regime where the parameter μ_r defines the onset of the tRSW which precedes the DL (along μ_d) and is bounded in between μ_r and μ_d. The region bounded between μ_d and $\mu_l = \mu_{sf}$ (μ_{sf}, offset of SSW) represents the SSW regime. The characteristic value $\mu = \mu_l$ defines the terminating solution (SSW in this case) for any kind of solitary wave. For the region beyond β_I, we have Type II transition where a new regime emerges depicting gVSW solutions. The lower bound of this new regime is marked by μ_{vi}. It is a sheer continuation of the μ_d curve prior to β_I and and replaces it for the current regime. The continuity of this boundary curve $\mu_d - \mu_{vi}$ further strengthens the idea that a gVSW is, indeed, a 'lost DL' which replaces DL solutions in the case of Type II transitions. The curve μ_{p-CoI} represents a $p - CoI$ solution which is the border line between the upper boundary of the gVSW and the onset of the SSW. Physically it implies transition of a gVSW to SSW via p-CoI. Starting from β_I, the μ_{p-CoI} curve bifurcates upward enlarging the gVSW regime with increasing β. Along with gVSW, the regime showing SSW solutions (lavender color) also enlarges as μ_l increases monotonically with β. It is to note that, for a Type II transition, the onset of a gVSW is now preceded by a set of tRSWs, just in the same way as it has previously preceded a DL for a Type I transition. This not only broadens the definition of a tRSW but also makes the onset of a gVSW as the apt substitute of a DL for a Type II transition.

In Fig. 9 we have plotted the $\mu - \beta$ regime of structures involved across β_{CoI}. At β_{CoI}, the terminating solution is an $n - CoI$, followed by a gVSW for $\beta > \beta_{CoI}$. In the figure $\mu_{ti}(\approx \mu_r)$ and $\mu_{tf}(\approx \mu_{vi})$ define the onset and offset of tRSW, respectively, whereas μ_{vf} ($\mu_n - CoI$) represents the offset of gVSW (SSW), respectively. β_I in Fig. 8. The μ_{n-CoI} bifurcates down from μ_l revealing an upper band of gVSWs (Persian green color). After $\beta = \beta_{CoI}$ we thus have two kinds of gVSWs. The one which precedes the SSW solution is the lower band of the gVSW, represented as $gVSW_m$ (apricot color) and the one after it is represented by the upper band of gVSWs (Persian green color) and is called $gVSW_a$. The characteristics of the upper (lower)

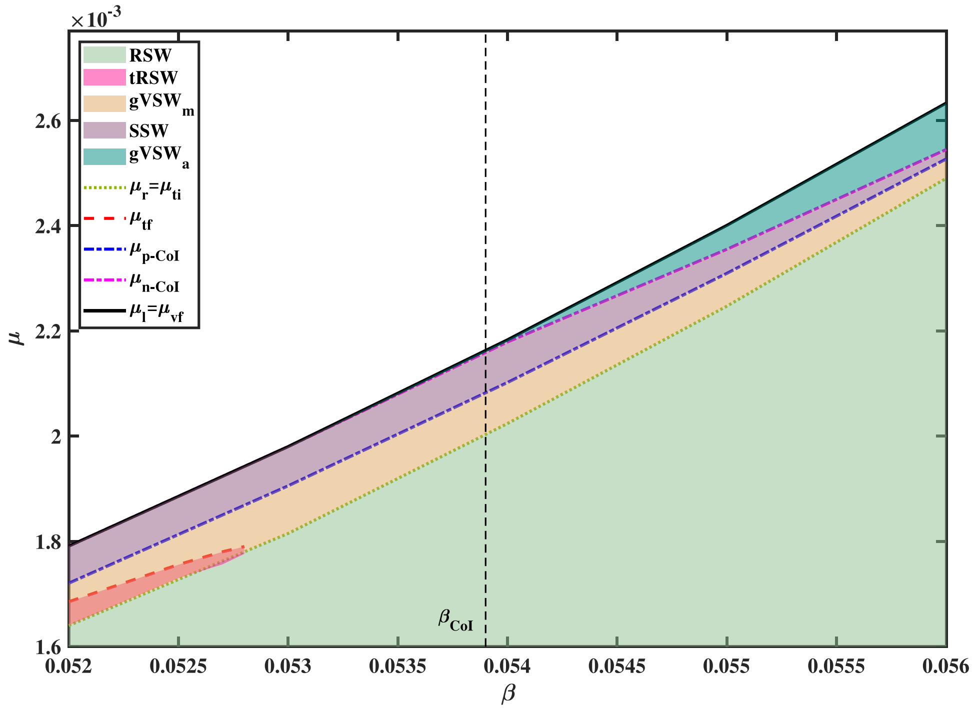

Fig. 9. The $\beta - \mu$ regime of nonlinear structures across β_{CoI}.

band of the gVSW solution, namely $gVSW_a$ ($gVSW_m$), is associated with that of the solid ($gVSW_a$) /dashed curve ($gVSW_m$) of Fig. 7, which are representing the corresponding Sagdeev pseudopotentials. Interestingly, as β increases, $\mu_{vi} \approx \mu_{tf}$ (the pink dashed line) decreases while $\mu_r \approx \mu_{ti}$ increases monotonically. Ultimately, beyond certain β value, the two merges together making tRSW one single boundary solution between RSW and gVSW. To distinguish its characteristics, and avoid any confusion later, we choose to denote that particular μ value as μ_t rather than μ_r (shown in Fig. 9). The trend continues further. Both μ_{n-CoI} and μ_{p-CoI} curves start converging to each other after crossing β_{CoI}, diminishing the existence domain of the SSW solution. Consequently, the lower band of gVSW, i.e., $gVSW_m$ (apricot color), also shrinks while the upper band representing $gVSW_a$ (Persian green color) expands with increasing β. The curves depicting μ_{p-CoI} and μ_{n-CoI} ultimately merge at β_{II} which is the final β value supporting SSW solutions.

The following figure (Fig. 10) marks the solutions across β_{II}. At the left side of β_{II}, μ_{p-CoI} and μ_{n-CoI} gradually converge, terminating the existence domain for SSW beyond β_{II}. Interestingly μ_t, too converges with them, eliminating the lower band of the gVSWs, namely $gVSW_m$. Beyond β_{II}, the regime shows only the upper band of gVSWs, viz., $gVSW_a$, while the tRSW (green dotted line) continues to be the boundary between the RSW and the $gVSW_a$. Upto β_v, the terminating solution remains the gVSW.

To complete the picture regarding the transition between nonlinear structures, in Fig. 11 we have plotted the $\beta - \mu$ regime of ENLSW across β_v. The parameter is defined as that β value, up to which, the terminating solution is a gVSW. The present, corrected value of $\beta_v \sim (= 0.0638)$ is estimated from the condition in Eq. 7b(b) and is much lower than the previous overestimated value of $\beta_v \sim (= 0.067)$ which resulted due to the misinterpretation of the gVSW solutions, as discussed in Section 2.4 [12]. This overestimation led us to beleive that there cannot be any RSW solution which may have a larger amplitude than the associated gVSW. However, Fig. 11 shows that, even after β_v there is a definite regime for gVSW where the terminating solution is now a tRSW which has a larger amplitude than the corresponding gVSW. Prior to β_v the lower limit of gVSW is, by and large, a tRSW. As β increases and approaches towards β_v, the curve representing tRSW solutions (i.e., $\mu = \mu_t$) crosses the gVSW regime and beyond β_v, it turns to be the upper limit of the gVSW. Instead of β_v the β value up to which the model supports OSWs is now termed as β_t. Between β_v and β_t the terminating solution is now a tRSW.

After β_t, the terminating solution ($\mu_l = \mu_n$) is a kind of RSW with negative $\frac{\partial^3\Psi}{\partial\Phi^3}$ and we called it as RSW_n. In order to differentiate it from that of tRSW and gVSW, in Fig. 12 we have plotted the Sagdeev pseudopotential profile and derivatives, of an RSW_n. It shows a smooth profile of Sagdeev pseudopotential (Fig. 12(a)) but its 1st derivative shows a definite wiggle (Fig. 12(b)). It means that, though there is no fluctuation in the charge separation (Δn), its rate of change varies. As a result, the 2nd order derivative is no more a monotonic one, though it still have a single root like an RSW (Fig. 12(c)). The variation leads to a negative 3rd order derivative as shown in Fig. 12(d). A VSW is defined by its fluctuating Δn while for both a tRSW and DL, it decreases near its maximum amplitude. For an RSW_n, on the contrary, there is no fluctuation in Δn and the number of roots for the second order derivative also remain the same as any typical RSW. In other words, according

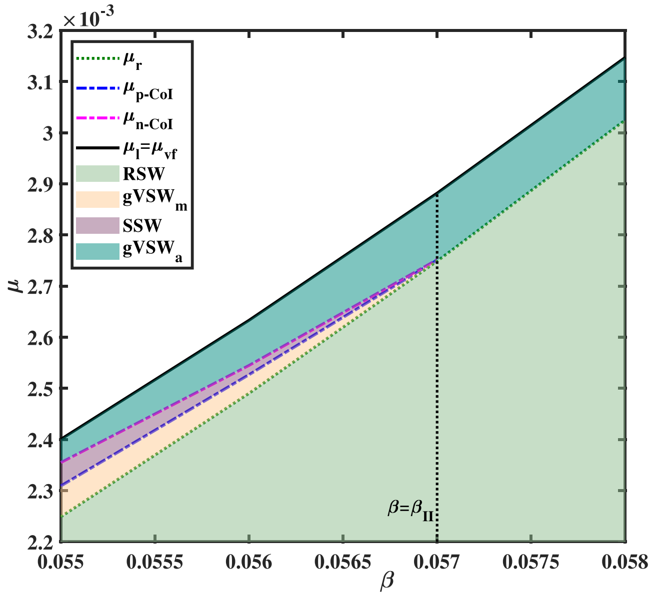

Fig. 10. The $\beta - \mu$ regime of nonlinear structures across β_{II}.

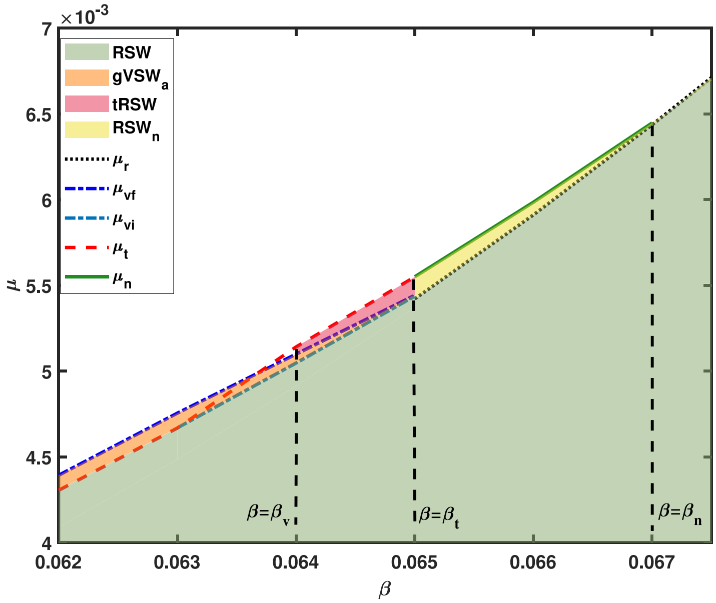

Fig. 11. The $\beta - \mu$ regime of nonlinear structures across β_v.

to all the conditions established so far, an RSW_n is indistinguishable from any typical RSW except for its negative 3rd order derivative. That's why we choose to categorize it as a regular solitary wave, with subscript "n" for its negative $\frac{\partial^3\Psi}{\partial\Phi^3}$. As β increases further, RSW_n will disappear retaining only the usual solitary wave solution.

To summarize, we may now claim that a negative value of 3rd derivative may denote an ENLSW, a transitional phase towards ENLSW, or an RSW near the vicinity of any ENLSW. However, though it is a necessary condition, but is not sufficient to categorise any particular type of ENLSW and they claim for additional conditions. On the other hand, the absence of any negative 3rd derivative is sufficient to identify an RSW but is not necessary. The condition may not hold good near the vicinity of an ENLSW in the parameter space. After a rigorous scrutiny of all the above mentioned structures, we have summarized their respective conditions and the definition of characteristic μ values in Table 1 and Table 2 respectively.

In this section, we have critically investigated the effect of the ambient density of the cooler component of cooler to hotter electrons and the temperature ratio of cooler to hotter electrons on the existence of various nonlinear structures in plasma. The relative temperature ratio and concentrations of the two electron components define the respective parameter

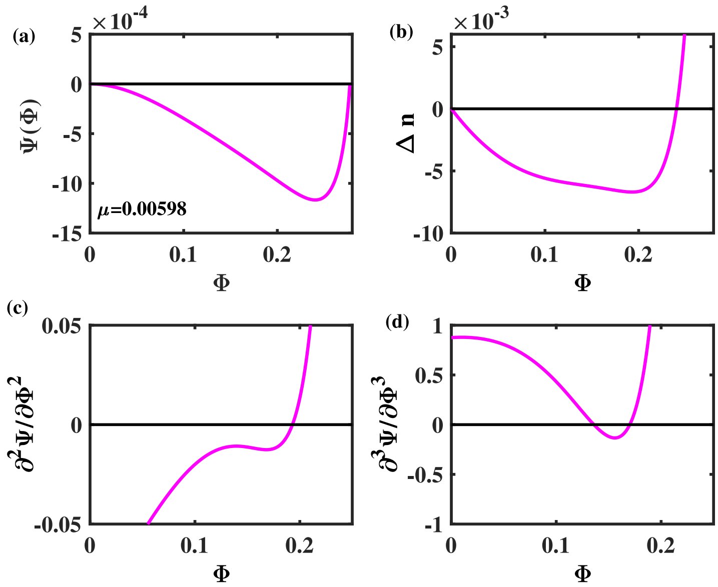

Fig. 12. (a) Sagdeev pseudopotential profile, (b) $\frac{\partial\Psi}{\partial\Phi}$ Vs Φ, (c) $\frac{\partial^2\Psi}{\partial\Phi^2}$ Vs Φ, and (d) $\frac{\partial^3\Psi}{\partial\Phi^3}$ Vs Φ for an RSW_n.

Table 1
Conditions for the existence of different types of solitary structures.

Nonlinear structures	Conditions			
	No. of extrema in $\Psi(\Phi)$	Number of roots in $\frac{\partial\Psi}{\partial\Phi}$	Number of roots in $\frac{\partial^2\Psi}{\partial\Phi^2}$	Number of roots in $\frac{\partial^3\Psi}{\partial\Phi^3}$
RSW ; RSW_n	2	2	1	Positive ; Positive & negative
tRSW	2	2	2	Positive & negative
gVSW	2	2	3	Positive & negative
CoI	2	3	3	Positive & negative
SSW	4	4	3	Positive & negative

Table 2
Definition of characteristic μ values.

Characteristic μ value	μ value for...
μ_d	DL solution, $\mu = \mu_d$
μ_r	onset of the negative value for $\frac{\partial^3\Psi}{\partial\Phi^3}$, $\mu > \mu_r$
μ_t	tRSW solution, $\mu = \mu_t$
μ_{ti}	onset of tRSW
μ_{tf}	offset of tRSW, $\mu_{ti} < \mu < \mu_{tf}$
μ_{vi}	onset of gVSW
μ_{vf}	offset of gVSW, $\mu_{vi} < \mu < \mu_{vf}$
μ_{p-Col}	p-CoI solution, $\mu = \mu_{p-\text{Col}}$
μ_{n-Col}	n-CoI solution, $\mu = \mu_{n-\text{Col}}$
μ_n	nRSW solution, $\mu = \mu_n$
μ_l	the terminating solution, $\mu = \mu_l$

regimes where the solutions exhibit distinctly different characteristics. This also highlights their sensitivity towards electron parameters and the key role played by the minority component of electrons. Due to the admixing of the ionospheric electrons, a magnetospheric plasma may be aptly described by the presence of a minority component of cooler electrons while for a laboratory plasma, they often occur due to filament heating or secondary emissions [5,16]. In reality, the temperature and density of this minority component may not remain constant but becomes variable which makes our analysis relevant for such cases.

Besides two electron temperature electrons, we have also assumed the presence of a minority component of alpha particles or He ions. This model is appropriate for the higher altitude of auroral region. This model is appropriate for the higher altitude of auroral region. Apart from the conventional solitary waves, this newly emerged theory of non-conventional, or extra nonlinear solitary waves would likely to have potential applications at different fields of plasma physics.

3. Conclusion

In the present paper, we have delineated the complete existence domain of ENLSWs intricately and quantitatively in a $\beta - \mu$ parameter space. In this process, we have quantified the onset and offset of each kinds of structures incorporating the derivative analysis. The transitional phase (tRSW) which separates ENLSWs from any regular solitary wave solutions (RSWs) is marked by a trough in Δn at its maximum amplitude, instead of a peak and can be termed as an 'incomplete DL'. This leads to a complete DL for a Type I transition preceding an SSW whereas for a Type II transition, it merges with a gVSW. A gVSW, on the other hand, is marked by its secondary compression after the trough of a tRSW, prior to its maximum amplitude, initiating the fluctuation in Δn. It is thus can aptly called as a 'lost DL'. The overall trend shows that, as β increases, a particular existence domain often shifts to a lower value of μ. Thus the spindle shaped existence domain of SSW shifts to lower μ for $\beta > \beta_{CoI}$, revealing the upper band of gVSW. Following the termination of SSW solutions, the two bands of gVSW merged together for $\beta > \beta_{II}$ and shifts to a lower μ for β_v, revealing an upper band of tRSW, where it denotes an offset of a gVSW rather than its onset. It is to note that, as β increases, transition paths from RSW to tRSW and tRSW to gVSW become so very gradual that it becomes very difficult to quantify them in details, and often they got mixed up for an upper β- upper μ regime. The overall existence domain of ENLSW terminates at β_t, followed by RSW_n which disappears beyond β_n.

Summarizing our overall analyses, we infer that an all positive $\frac{\partial^3\Psi}{\partial\Phi^3}$ not only ensures an RSW solution but also eradicates any possibility of ENLSW solution at its vicinity in the parameter space. On the other hand, to identify any specific kind of ENLSW one needs to study the roots of 1st and 2nd order derivatives as well. Both tRSW and RSW_n, denoting the transitional phase to ENLSW (tRSW), or lying near its termination (RSW_n), satisfy the condition of Eq. (7b) though the latter remain indistinguishable from any typical RSW solution as per all other mathematical conditions described in Table 1

Author contributions

S. V. Steffy developed the theory, did the analytical part and perform computation. S. S. Ghosh verified the analytical part and supervised the findings of this work. Both the authors discussed the results and contributed to the final manuscript.

Declaration of Competing Interest

The authors declare that they have no known competing financial interests or personal relationships that could have appeared to influence the work reported in this paper.

CRediT authorship contribution statement

Steffy Sara Varghese: Conceptualization, Data curation, Formal analysis, Validation, Writing - original draft. **S.S. Ghosh:** Supervision, Writing - review & editing.

References

[1] Varghese SS, Ghosh SS. Phys Plasmas 2016;23(8):082304. doi:10.1063/1.4959851.
[2] Dubinov AE, Kolotkov DY. IEEE TPS 2012;40(5):1429–33. doi:10.1109/TPS.2012.2189026.
[3] Steffy SV, Ghosh SS. Phys Plasmas 2018;25(6):062302. doi:10.1063/1.5033503.
[4] Dubinov AE, Kolotkov DY. Plasma Phys Rep 2012;38(11):909–12. doi:10.1134/S1063780X12100054.
[5] Ghosh SS, Ghosh KK, Sekar Iyengar AN. Phys Plasmas 1996;3(11):3939–46. doi:10.1063/1.871567.
[6] Olivier CP, Verheest F, Maharaj SK. J Plasma Phys 2017;83(6):905830605. doi:10.1017/S0022377817000848.
[7] Kakad A, Lotekar A, Kakad B. Phys Plasmas 2016;23(11):110702. doi:10.1063/1.4969078.
[8] Olivier CP, Verheest F, Hereman WA. Phys Plasmas 2018;25(3):032309. doi:10.1063/1.5027448.
[9] Lotekar A, Kakad A, Kakad B. Phys Plasmas 2019;26(10):100701. doi:10.1063/1.5119993.
[10] Dubinov A, Kolotkov D. High Energy Chem 2012;46:0018–1439. doi:10.1134/S0018143912060033.
[11] Dubinov A, Kolotkov D. Rev Mod Plasma Phys 2018;2(2):2367–3192. doi:10.1007/s41614-018-0014-9.
[12] Varghese SS, Ghosh SS. Phys Plasmas 2017;24(10):102111. doi:10.1063/1.4993511.
[13] Verheest F, Hellberg MA, Kourakis I. Phys Rev E 2013;87. doi:10.1103/PhysRevE.87.043107.
[14] Hellberg MA, Baluku TK, Verheest F, Kourakis I. J Plasma Phys 2013;79(6):1039–43. doi:10.1017/S0022377813001153.
[15] Varghese SS, Ghosh SS. Phys Plasmas 2018;25(1):012307. doi:10.1063/1.5006972.
[16] Jones WD, Lee A, Gleman SM, Doucet HJ. Phys Rev Lett 1975;35:1349–52. doi:10.1103/PhysRevLett.35.1349.